

## Supporting Information

### Cyanocarbazole-based bipolar host materials for efficient phosphorescent and thermally activated delayed fluorescent OLEDs

Yeting Tao,<sup>a</sup> Yaotian Zhang,<sup>a</sup> Shiying Hu,<sup>a</sup> Jian Wang,<sup>a</sup> Yuying Wu,<sup>a</sup> Wenbo Yuan,<sup>\*a</sup> Wei Yao,<sup>a,b</sup> and Youtian Tao<sup>\*a</sup>

#### Experimental section

##### Materials

All the reagents were purchased from Energy Chemical Co. and Sinopharm Chemical Reagent Co. without further purification. All the solvents were used as received from Nanjing WANQING chemical Glass ware & Instrument Co. and J&K Scientific.

##### General procedures

<sup>1</sup>H NMR spectra were recorded on a Bruker DMX-500 spectrometer in deuteriochloroform using tetramethylsilane (TMS;  $\delta = 0$  ppm) as an internal standard. Mass spectra were recorded using a Bruker Autoflex matrix assisted laser desorption/ionization time-of-flight (MALDI-TOF) and Waters Xevo-TQ Ultra performance liquid chromatogram Tandem Quadrupole Mass Spectrometry (LC-MS). Elemental analyses (EA) of C, H, N, and S were performed on a Vario EL III microanalyzer. Absorption spectra: Ultraviolet-visible (UV-Vis) absorption spectra of solution in dichloromethane and thin film on a quartz substrate were measured using Shimadzu UV-2500 recording spectrophotometer, and the photoluminescence (PL) spectra were recorded using a Hitachi F-4600 fluorescence spectrophotometer. Thermal gravimetric analysis (TGA) was undertaken with a METTLER TOLEDO TGA2 instrument. The thermal stability of the samples was determined by measuring their weight loss at a heating rate of 10°C min<sup>-1</sup> from 25 to 500°C using 3 mg sample under a nitrogen atmosphere. Differential scanning calorimetry (DSC) was performed on a NETZSCH DSC 200 PC unit within the temperature range of 50 to 300°C, heating at a rate of 10°C min<sup>-1</sup> under N<sub>2</sub> atmosphere. Cyclic voltammetry (CV): The electrochemical cyclic voltammetry was conducted on a CHI voltammetric analyzer, in a 0.1 mol L<sup>-1</sup> acetonitrile solution of tetrabutylammonium hexafluorophosphate (n-Bu<sub>4</sub>NPF<sub>6</sub>) at a potential scan rate of 100 mV s<sup>-1</sup>. The conventional three electrode configuration consists of a platinum working electrode, a platinum wire counter electrode, and an Ag/AgCl wire pseudo-reference electrode. The polymer sample was coated on the platinum sheet of working electrode. The reference electrode was checked versus ferrocenium-ferrocene (Fc<sup>+</sup>/Fc) as internal standard as recommended by IUPAC (the vacuum energy level: 24.8 eV). All the solutions were deaerated by bubbling nitrogen gas for a few minutes prior to the electrochemical measurements. HOMO energy levels were calculated from the equation of  $E_{\text{HOMO}} = -(E_{\text{onset}}(\text{ox}) + 4.8)$  eV, and LUMO energy levels were deduced from the optical band gap ( $E_{\text{g}}$ ) values and HOMO levels.

##### OLED fabrication and measurements

The electroluminescent devices were fabricated by vacuum deposition technology, and all functional layers were fabricated on pre-treated indium tin oxide (ITO) substrates. ITO glass substrates were successively cleaned by

ultrasonic wave with detergent, alcohol, acetone and deionized water, then dried at 120°C in a vacuum oven for more than 60 min. The structure of the TADF device was ITO/HAT-CN (3 nm)/TAPC (40 nm)/TCTA (5 nm)/mCP (5 nm)/EML (20 nm)/TmPyPB (40 nm)/Liq (1 nm)/Al(100 nm). Firstly, 3 nm of dipyrzino[2,3-*f*:2',3'-*h*]quinoxaline-2,3,6,7,10,11-hexacarbonitrile (HAT-CN) was deposited on ITO substrates as hole injection layer, followed by 40 nm of 4,4'-cyclohexylidenebis[*N,N*-bis(4-methylphenyl)aniline] (TAPC) and 5 nm of *N,N,N*-tris[4-(9-carbazolyl)phenyl]amine (TCTA) and 5 nm of 9,9'-(1,3-Phenylene)bis-9*H*-carbazole (mCP) as hole transporting layer. Finally, the electron transporting layer was 1,3,5-tri(m-pyrid-3-ylphenyl)benzene (TmPyPB) for 40 nm, meanwhile, the 1 nm of Liq and hundred-nanometer of Al were considered as the cathode layers. Current density-voltage-luminance (*J-V-L*) characteristics were tested through using a Keithley source measurement unit (Keithley 2400 and Keithley 2000) and a calibrated silicon photodiode. In addition, the EL spectra were measured by a Spectra scan PR650 spectrophotometer. It should be noted that the measurements were carried out at room temperature under ambient condition.

## Computational details

The calculations were performed with the Gaussian 09 package, using the density functional theory (DFT) and time-dependent density functional theory (TD-DFT) method with the PBE0 functional.<sup>[1-3]</sup> The structures were optimized using DFT (*S*<sub>0</sub> state) or TD-DFT (*S*<sub>1</sub> and *T*<sub>1</sub> state) methods with a 6-31G(d) basis set. Natural transition orbital analyses<sup>[4]</sup> were also performed to examine the nature of the excited states and the orbit visualization was realized using the Multiwfn software.<sup>[5]</sup>

## Synthesis of compounds

### ***9-(2-(4,6-diphenyl-1,3,5-triazin-2-yl)phenyl)-9H-carbazole-3-carbonitrile (o-3CN-TRZ)***

A mixture of 2-(2-fluorophenyl)-4,6-diphenyl-1,3,5-triazine (500.0 mg, 1.53 mmol), 9*H*-carbazole-3-carbonitrile (352.3 mg, 1.83 mmol) and K<sub>2</sub>CO<sub>3</sub> (633.3 g, 4.58 mmol) in dimethyl sulfoxide (DMSO) (15 mL) was stirred at 150°C for 20 h under an N<sub>2</sub> atmosphere. After cooling to room temperature, the mixture was poured into water, filtered, and then purified by column chromatography over silica gel with ethyl acetate/petroleum ether as the eluent to afford white solid (Yield: ~76%). <sup>1</sup>H NMR (400 MHz, CDCl<sub>3</sub>): δ ppm 8.62-8.57 (m, 1H), 8.31 (dd, *J*=1.6, 0.7 Hz, 1H), 8.03 (dt, *J*=7.8, 1.0 Hz, 1H), 8.00-7.95 (m, 4H), 7.89-7.79 (m, 2H), 7.70-7.65 (m, 1H), 7.57 (dt, *J*=8.6, 1.2 Hz, 1H), 7.48 (ddt, *J*=8.7, 7.0, 1.2 Hz, 2H), 7.41 (ddt, *J*=8.3, 7.2, 1.0 Hz, 1H), 7.35-7.28 (m, 5H), 7.25-7.21 (m, 2H). <sup>13</sup>C NMR (101 MHz, CDCl<sub>3</sub>): δ ppm 171.69, 171.44, 143.57, 142.62, 136.16, 135.49, 135.27, 133.11, 132.86, 132.70, 130.45, 129.75, 129.32, 128.73, 128.49, 127.58, 125.31, 123.67, 122.33, 121.01, 120.71, 120.61, 110.52, 110.35, 102.31. MALDI-TOF Mass (*m/z*): calcd for C<sub>34</sub>H<sub>21</sub>N<sub>5</sub>: 499.58; found: 500.19 [H<sup>+</sup>]. Anal. Calculated for C<sub>34</sub>H<sub>21</sub>N<sub>5</sub>: C 81.74, H 4.24, N 14.02%; found: C 81.72, H 4.21, N 14.15%.

### ***9-(2-(4,6-diphenyl-1,3,5-triazin-2-yl)phenyl)-9H-carbazole-4-carbonitrile (o-4CN-TRZ)***

A mixture of 2-(2-fluorophenyl)-4,6-diphenyl-1,3,5-triazine (500.0 mg, 1.53 mmol), 9*H*-carbazole-4-carbonitrile (352.3 mg, 1.83 mmol) and K<sub>2</sub>CO<sub>3</sub> (633.3 g, 4.58 mmol) in dimethyl sulfoxide (DMSO) (15 mL) was stirred at 150°C for 20 h under an N<sub>2</sub> atmosphere. After cooling to room temperature, the mixture was poured into water, filtered, and then purified by column chromatography over silica gel with ethyl acetate/petroleum ether as the eluent to afford white solid (Yield: ~72%). <sup>1</sup>H NMR (400 MHz, DMSO), δ (TMS, ppm): δ 8.62 (d, *J*=9.2 Hz), 8.33 (d, *J*=7.6 Hz), 8.02 (t, *J*=7.6 Hz), 7.97-7.88 (m), 7.73 (dd, *J*<sub>1</sub>=6.2, *J*<sub>2</sub>=2.2 Hz), 7.58 (t, *J*=7.4 Hz), 7.55-7.49 (m), 7.47-7.31 (m), 7.17 (d, *J*=7.8 Hz). <sup>13</sup>C NMR (101 MHz, CDCl<sub>3</sub>): δ ppm 171.63, 171.44, 142.45, 141.49, 136.00, 135.68, 135.28, 133.16, 132.89, 132.73, 130.68, 129.61, 128.69, 128.51, 128.03, 125.50, 124.64, 123.80, 121.88, 121.18, 120.73, 118.85, 114.24, 110.09, 103.82. MALDI-TOF Mass (*m/z*): calcd for C<sub>34</sub>H<sub>21</sub>N<sub>5</sub>: 499.58; found: 500.19 [H<sup>+</sup>]. Anal. Calculated for C<sub>34</sub>H<sub>21</sub>N<sub>5</sub>: C 81.74, H 4.24, N 14.02%; found: C 81.49, H 4.34, N 14.03%.

## Figures and tables

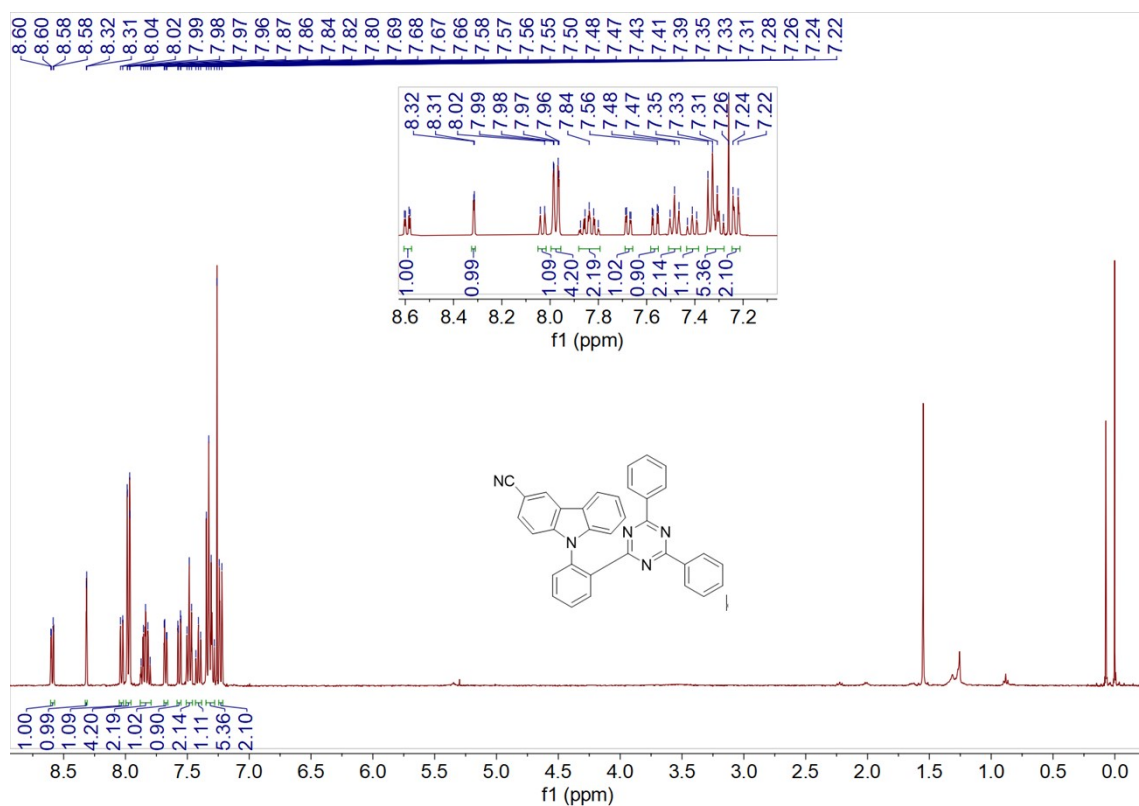


**Figure S1.** <sup>1</sup>H NMR spectra for compound *o*-3CN-TRZ.

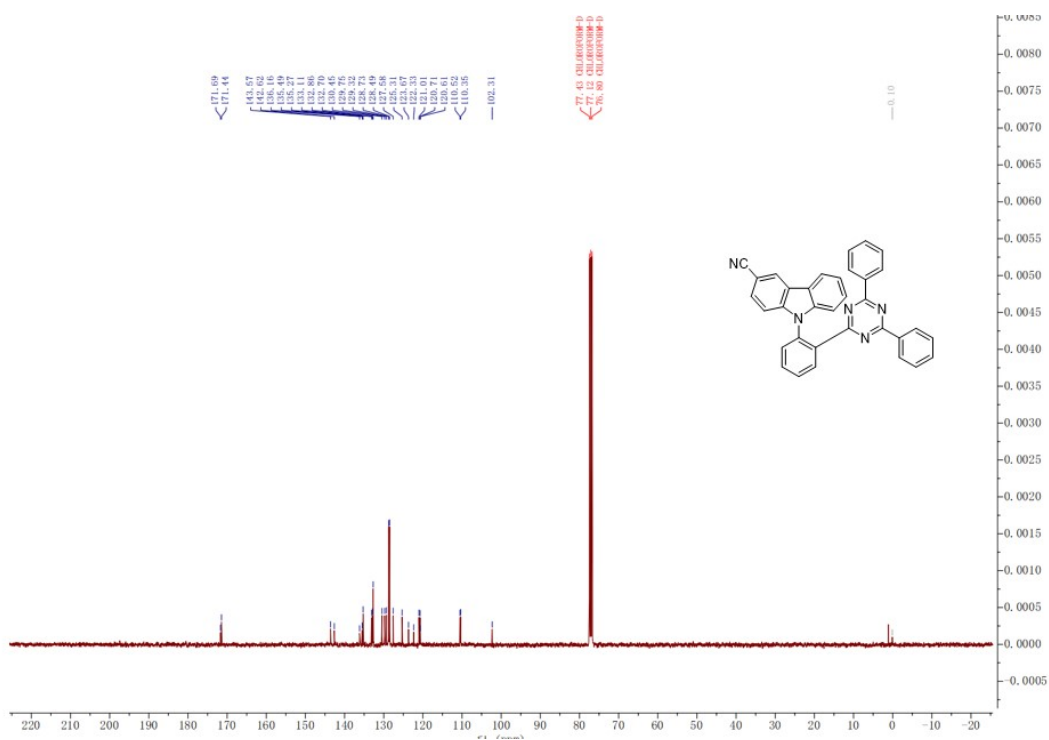


**Figure S2.**  $^{13}\text{C}$  NMR spectra for compound *o*-3CN-TRZ.

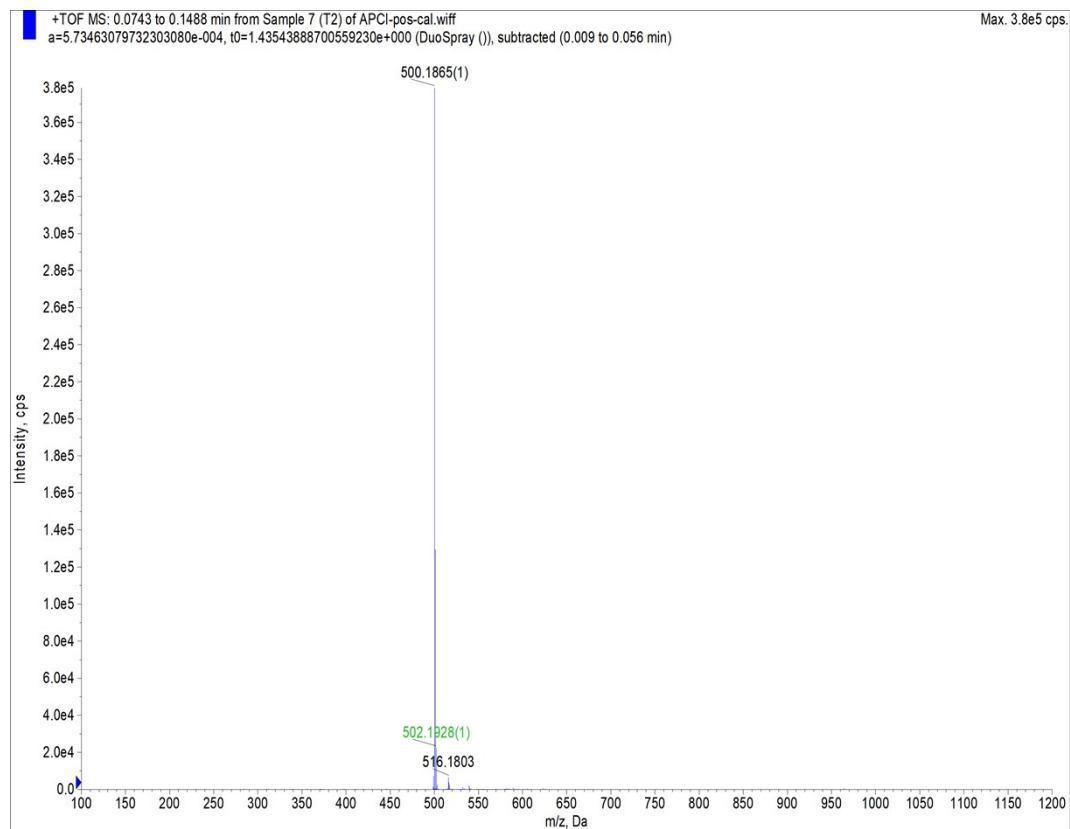


**Figure S3.** MALDI-TOF Mass spectrometry for compound *o*-3CN-TRZ.

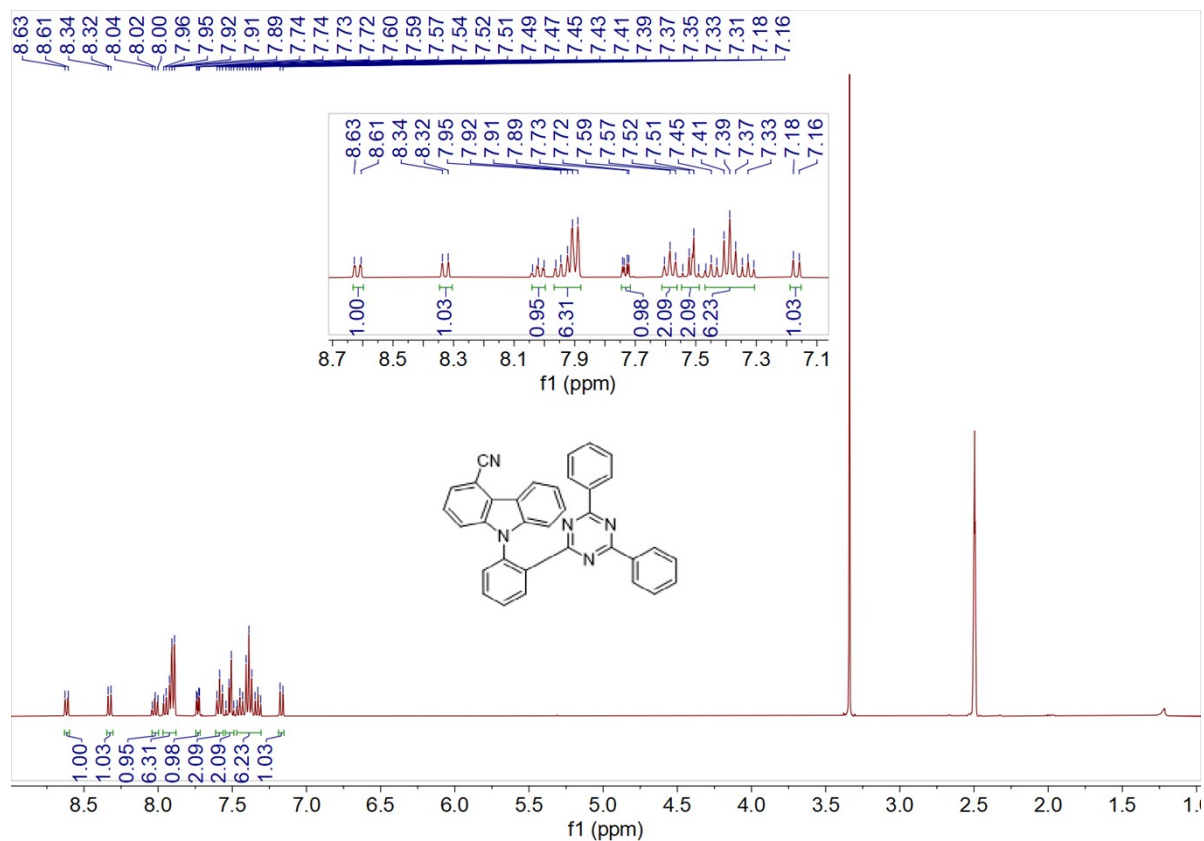


Figure S4. <sup>1</sup>H NMR spectra for compound *o*-4CN-TRZ.

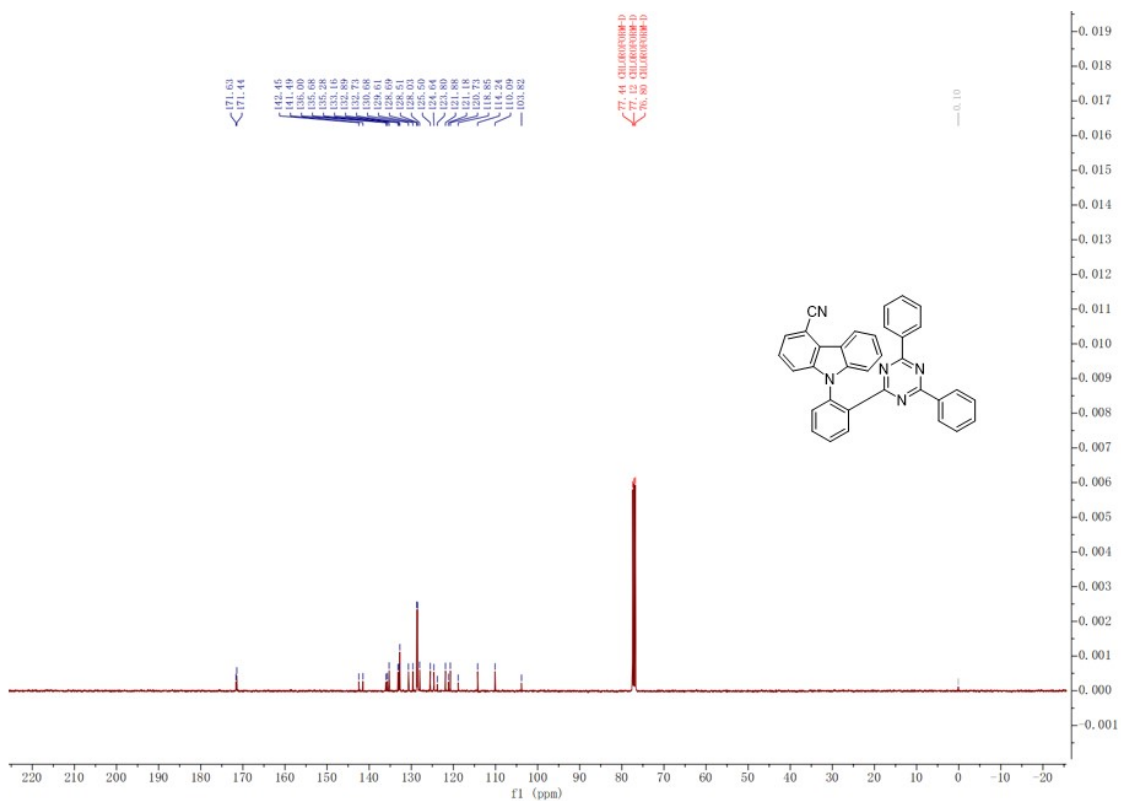
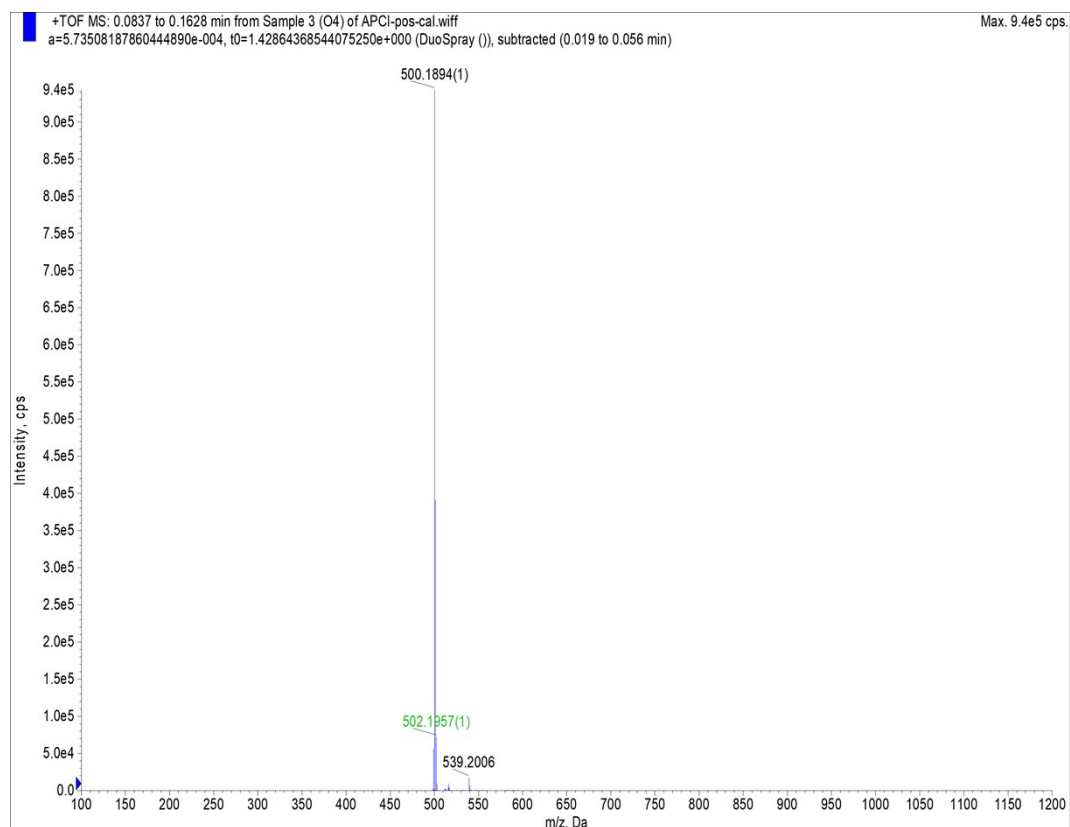
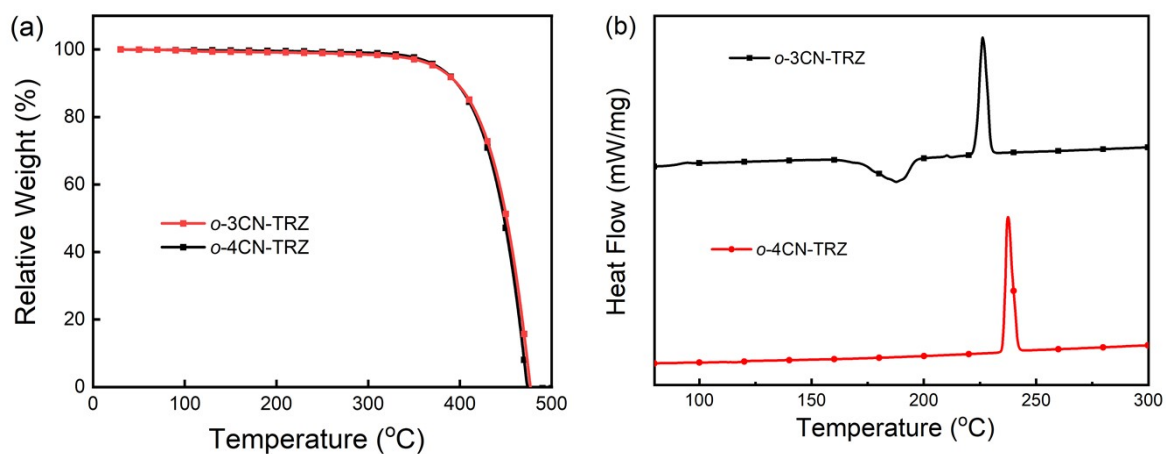


Figure S5. <sup>13</sup>C NMR spectra for compound *o*-4CN-TRZ.



**Figure S6.** MALDI-TOF Mass spectrometry for compound *o*-4CN-TRZ.



**Figure S7.** (a) Thermogravimetric analysis (TGA) and (b) differential scanning calorimetry (DSC) curves for *o*-3CN-TRZ and *o*-4CN-TRZ.

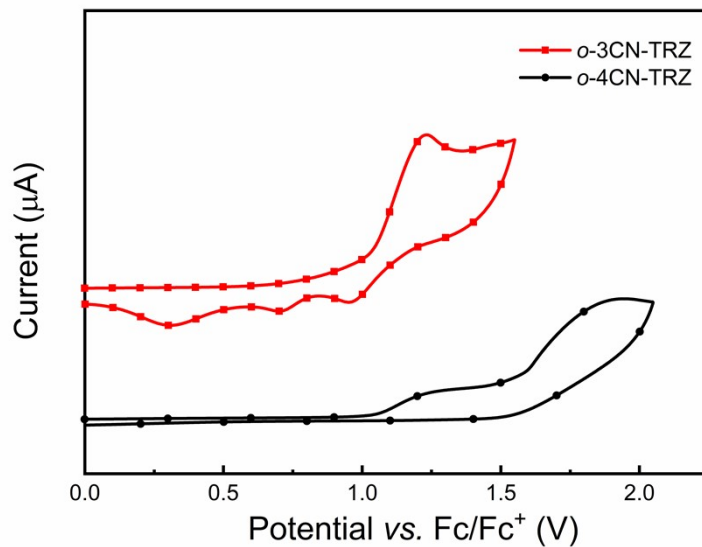


**Figure S8.** Oxidation curves of *o*-3CN-TRZ and *o*-4CN-TRZ by cyclic voltammetry.

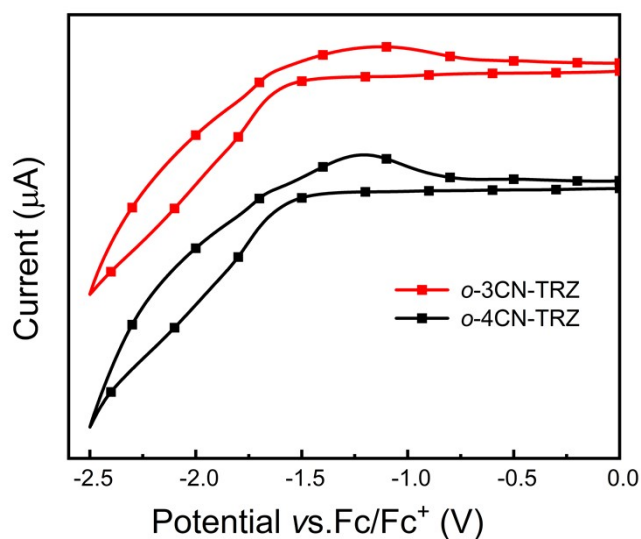


**Figure S9.** Reduction curves of *o*-3CN-TRZ and *o*-4CN-TRZ by cyclic voltammetry.

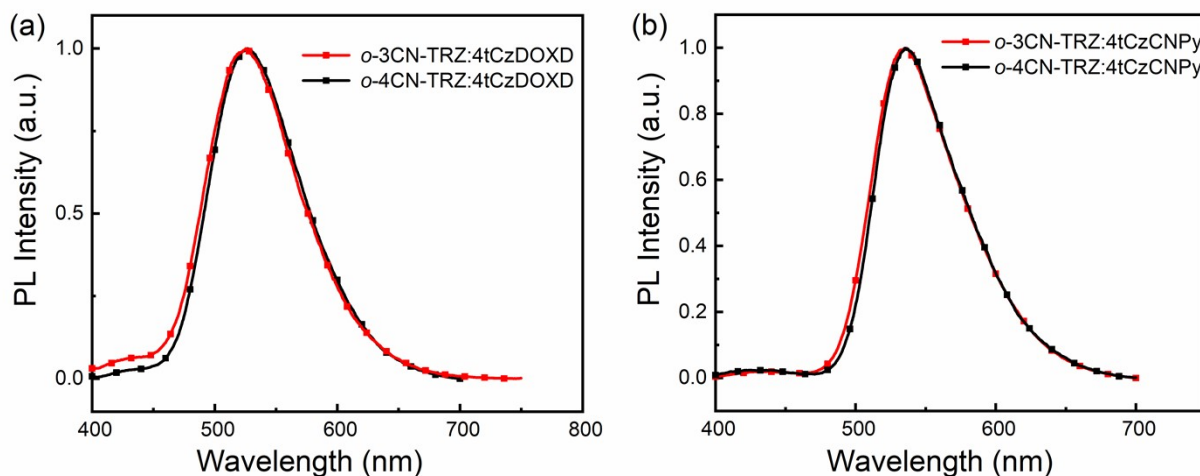


**Figure S10.** The PL spectra of the doped films: (a) *o*-3CN-TRZ or *o*-4CN-TRZ host: 10 wt% 4tCzDOXD, (b) *o*-3CN-TRZ or *o*-4CN-TRZ: 10 wt% 4tCzCNPy.

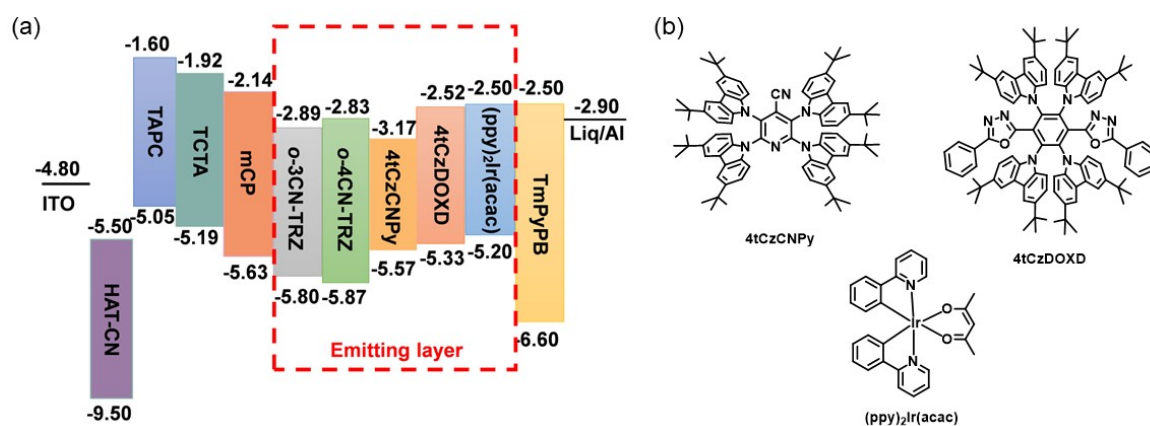


**Figure S11.** (a) The energy level diagrams and device structures for device A-F, (b) the chemical structure of the relevant dopants.

**Table S1.** The summary of lifetime, PLQYs and rate constants of the doped films.

Host	Dopant	$\tau_p$ (ns)	$\tau_d$ ( $\mu$ s)	PLQY (%)	$k_F$ ( $\times 10^7$ s <sup>-1</sup> )	$k_{ISC}$ ( $\times 10^8$ s <sup>-1</sup> )	$k_{RISC}$ ( $\times 10^6$ s <sup>-1</sup> )
<i>o</i> -3CN-TRZ	4tCzDOXD	4.95	1.91	70	1.5	1.9	4.8
	4tCzCNPy	1.79	3.77	61	3.3	5.3	1.5
<i>o</i> -4CN-TRZ	4tCzDOXD	6.16	1.79	76	1.4	1.5	4.9
	4tCzCNPy	1.67	3.63	78	8.4	5.1	2.6



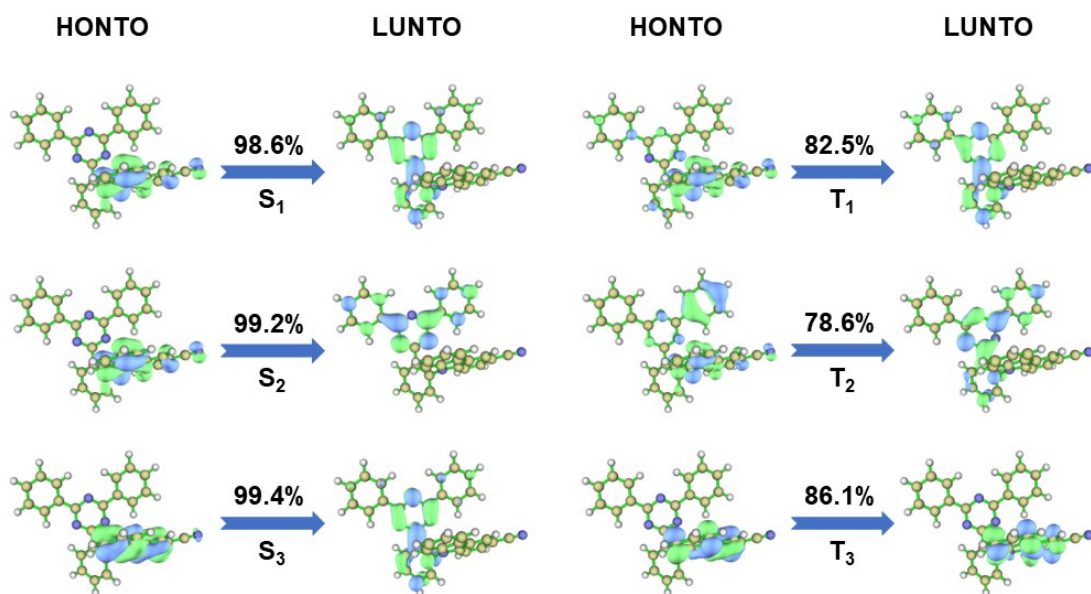


**Figure S12.** The natural transition orbitals of *o*-3CN-TRZ.

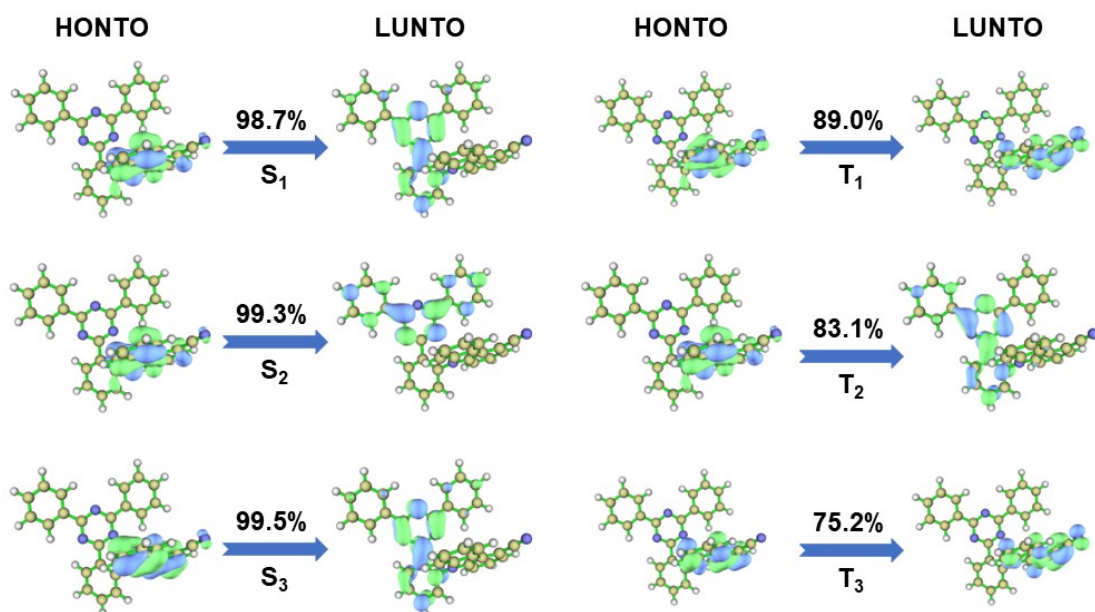


**Figure S13.** The natural transition orbitals of *o*-4CN-TRZ.

## References

1. A. D. Becke, Density-functional exchange-energy approximation with correct asymptotic behavior, *Phys. Rev. A*, 1988, 38, 3098-3100.
2. C. Lee, W. Yang, R.G. Parr, Development of the Colle-Salvetti correlation-energy formula into a functional of the electron density, *Phys. Rev. B*, 1988, 37, 785-789.
3. H. Sun, C. Zhong, J. L. Brédas, Reliable Prediction with Tuned Range-Separated Functionals of the Singlet–Triplet Gap in Organic Emitters for Thermally Activated Delayed Fluorescence, *J. Chem. Theory. Comput.*, 2015, 11, 3851-3858.
4. Martin, R. L. Natural transition orbitals. *J. Chem. Phys.*, 2003, 118, 4775-4777.
5. T. Lu, F. Chen, Multiwfn: A multifunctional wavefunction analyzer, *J. Comput. Chem.* 2012, 33, 580-592.